QCD Mini Project: Beyond the RWA

Benjamin Sanders, Samuel Gabe

January 20, 2023

Abstract

The Jaynes-Cummings model provides a useful model to describe the interaction between a two-level atom coupled to a quantum harmonic oscillator. This model uses the rotating wave approximation (RWA) to simplify the analytical expression for the Hamiltonian of the system which allows for analytical solutions to be found and compared to experimental results. However, with experiments being able to produce increased coupling strength the rotating wave approximation becomes a poor approximation. We analyse the Hamiltonian numerically when both using the RWA and when not using the RWA to find its eigenvalues and how a system evolves in time when under the action of the Hamiltonian. We examine the cases for which the RWA is a good approximation and how the system evolves for the full Hamiltonian when the RWA breaks down. Our results concur with other theoretical results and will likely find use in the near future as coupling strengths increase.

Introduction

The Jaynes-Cummings model [1] describes a quantum system involving a two level atom coupled to a quantum harmonic oscillator. The Jaynes-Cummings model makes use of the rotating wave approximation (RWA) which simplifies the Hamiltonian of the system from an equation that remains to be solved analytically to one that not only been solved but has had a great amount of study and is explored in detail in text books [2]. If we start a system at some number state, n, in the excited state, $|e\rangle |n\rangle$, we know that the system will oscillate between the initial state and the the ground state of the number state above $|g\rangle |n+1\rangle$. The probability of finding the system in the excited state after some time, t, is analytically given by [2]

$$P_e(t) = \cos^2(\lambda\sqrt{n+1}t) \tag{1}$$

where λ is the coupling strength between the two level atom and the harmonic oscillator, meaning the frequency of this wave is proportional to $\lambda\sqrt{n+1}$. This model is very helpful for most of the current experimental work being done in this field.

However, as experimental circuits become more refined we are seeing systems with increasing coupling to the point where the Jaynes-Cummings model may no longer hold and we have to use a non-RWA approach. An important parameter to consider is the ratio of the coupling strength to the frequency, ω_a of the harmonic oscillator, $\frac{\lambda}{\omega_a}$. Interesting theoretical behaviour when not using the RWA has been shown by Larson [3] at $\frac{\lambda}{\omega_a} = 2$ whereby the probability of finding the system in an excited state collapses then recovers and resembles a wave-packet form, which notably does not match in the theoretical analysis for the Jaynes-Cummings model. While experiments are yet to show this behavior, there are a vast number of experiments that can produce strong coupling using various methods [4, 5] and one experiment has reached $\frac{\lambda}{\omega_a} = 1.34$ [6]. It is important therefore, for research to be done to establish the theoretical behaviour of such systems in stronger coupling regimes. Some such analysis has been done by Irish [7] which sought to make a generalised form of the RWA which still held for large coupling strengths.

This paper seeks to theoretically analyse how the system behaves both using and not using the RWA to ascertain the range of $\frac{\lambda}{\omega_a}$ values for which the RWA is a good approximation. We will also seek to reproduce the collapse and revival behaviour seen in Larson [3] for both cases to demonstrate a significant case where the Jaynes-Cummings model breaks down. This report will focus on the on-resonance case, i.e. where the frequencies of the atom and the harmonic oscillator are equal.

Method

The equation for the Hamiltonian, H, of the coupled two level atom and harmonic oscillator system is given by [2]

$$H = \hbar\omega a^\dagger a + \frac{\hbar\omega_a}{2}\sigma_z + \hbar\lambda(\sigma_+ + \sigma_-)(a^\dagger + a) \tag{2}$$

where ω is the transition frequency of the atom, ω_a is the frequency of the harmonic oscillator, $a^\dagger$ is the creation operator, a is the annihilation operator,$\sigma_z = |e\rangle\langle e| - |g\rangle\langle g|$, $\sigma_+ = |e\rangle\langle g|$ and $\sigma_- = |g\rangle\langle e|$. When making the RWA we drop the $\sigma_+ a^\dagger$ and $\sigma_- a$ terms and we end up with the Jaynes-Cummings model Hamiltonian, H_{JC} which is

$$H_{JC} = \hbar\omega a^\dagger a + \frac{\hbar\omega_a}{2}\sigma_z + \hbar\lambda(\sigma_+ a + \sigma_- a^\dagger) \tag{3}$$

Since there are currently no analytical solutions to the full Hamiltonian we will be using numerical methods in order to analyse the behaviour of the Hamiltonian for both the case when making the RWA and when not. This was done by representing the Hamiltonian in matrix form using a finite matrix that could be used in computational analysis. The form of the matrix that we used is shown in equation 4

$$H = \begin{pmatrix} \langle m|\langle g|H|g\rangle|mm\rangle & \langle m|\langle g|H|e\rangle|mm\rangle \\ \langle m|\langle e|H|g\rangle|mm\rangle & \langle m|\langle e|H|e\rangle|mm\rangle \end{pmatrix} \tag{4}$$

where each element represents a $n+1\times n+1$ matrix containing all of the matrix elements corresponding to the given combination of state type bra and ket. Each of these matrices will take the same form

$$\langle m|\langle i|H|ii\rangle|mm\rangle = \begin{pmatrix} \langle 0|\langle i|H|ii\rangle|0\rangle & \langle 0|\langle i|H|ii\rangle|1\rangle & \langle 0|\langle i|H|ii\rangle|2\rangle & \dots & \langle 0|\langle i|H|ii\rangle|n\rangle \\ \langle 1|\langle i|H|ii\rangle|0\rangle & \langle 1|\langle i|H|ii\rangle|1\rangle & \langle 1|\langle i|H|ii\rangle|2\rangle & \dots & \langle 1|\langle i|H|ii\rangle|n\rangle \\ \langle 2|\langle i|H|ii\rangle|0\rangle & \langle 2|\langle i|H|ii\rangle|1\rangle & \langle 2|\langle i|H|ii\rangle|2\rangle & \dots & \langle 2|\langle i|H|ii\rangle|n\rangle \\ \vdots & \vdots & \vdots & \ddots & \vdots \\ \langle n|\langle i|H|ii\rangle|0\rangle & \langle n|\langle i|H|ii\rangle|1\rangle & \langle n|\langle i|H|ii\rangle|2\rangle & \dots & \langle n|\langle i|H|ii\rangle|n\rangle \end{pmatrix} \tag{5}$$

where $\langle i|$ is either $\langle g|$ or $\langle e|$ and $|ii\rangle$ is either $|g\rangle$ or $|e\rangle$. In order to obtain numerical values for each element we must consider how the equation for the Hamiltonian in equation 2 acts on any given matrix element. We find that any matrix element for which the number states are equal and the state types are the same, the eigenenergy is given by

$$\langle n|\langle i|H|i\rangle|n\rangle = E_{n,\pm} = \hbar\omega n \pm \frac{\hbar\omega_a}{2} \tag{6}$$

with $E_{n,-}$ corresponding to terms involving the ground state and $E_{n,+}$ corresponding to terms involving the excited state. In this report we are looking exclusively at the on resonance case where $\omega = \omega_a$ so these eigenenergies simplify to

$$E_{n,\pm} = \hbar\omega_a\left(n \pm \frac{1}{2}\right) \tag{7}$$

These eigenenergies result from the first two terms in the equation for the Hamiltonian and are the same for both the full Hamiltonian and the Jaynes-Cummings model Hamiltonian. The final term in the Hamiltonian represents the interaction between the two level atom system and the harmonic oscillator. The rules set out in equation 8 allow us to complete the full Hamiltonian matrix by checking each remaining matrix element to see if it follows any of the rules and if so assign the corresponding value. If the remaining matrix elements do not follow any of the rules set out in equation 8 then we can set these values to zero as the Hamiltonian operator has no interaction on these states. For the matrix when using the RWA we refer back to equation 3 and set the matrix elements in 8a and 8d to zero, since these terms are not present in 3, leaving us with the terms in 8b and 8c. Hence we can see if a system starts in the $|e\rangle|n\rangle$ state we would expect it to be confined to the initial state and the $|g\rangle|n+1\rangle$.

$$\langle n-1|\langle g|H|e\rangle|n\rangle = \sqrt{n}\hbar\lambda \tag{8a}$$
$$\langle n-1|\langle e|H|g\rangle|n\rangle = \sqrt{n}\hbar\lambda \tag{8b}$$
$$\langle n+1|\langle g|H|e\rangle|n\rangle = \sqrt{n+1}\hbar\lambda \tag{8c}$$
$$\langle n+1|\langle e|H|g\rangle|n\rangle = \sqrt{n+1}\hbar\lambda \tag{8d}$$

Using the matrix elements determined above we formed matrices for full Hamiltonian and the Hamiltonian using the RWA. Examples for an 8×8 matrix for the full Hamiltonian and the Jaynes-Cumming Hamiltonian can be seen in equations 9 and 10 respectively.

$$H = \hbar\omega_a \begin{pmatrix} -\frac{1}{2} & 0 & 0 & 0 & 0 & \frac{\lambda}{\omega_a} & 0 & 0 & \dots \\ 0 & \frac{1}{2} & 0 & 0 & \frac{\lambda}{\omega_a} & 0 & \frac{\lambda\sqrt{2}}{\omega_a} & 0 & \dots \\ 0 & 0 & \frac{3}{2} & 0 & 0 & \frac{\lambda\sqrt{2}}{\omega_a} & 0 & \frac{\lambda\sqrt{3}}{\omega_a} & \dots \\ 0 & 0 & 0 & \frac{5}{2} & 0 & 0 & \frac{\lambda\sqrt{3}}{\omega_a} & 0 & \dots \\ 0 & \frac{\lambda}{\omega_a} & 0 & 0 & \frac{1}{2} & 0 & 0 & 0 & \dots \\ \frac{\lambda}{\omega_a} & 0 & \frac{\lambda\sqrt{2}}{\omega_a} & 0 & 0 & \frac{3}{2} & 0 & 0 & \dots \\ 0 & \frac{\lambda\sqrt{2}}{\omega_a} & 0 & \frac{\lambda\sqrt{3}}{\omega_a} & 0 & 0 & \frac{5}{2} & 0 & \dots \\ 0 & 0 & \frac{\lambda\sqrt{3}}{\omega_a} & 0 & 0 & 0 & 0 & \frac{7}{2} & \dots \\ \vdots & \vdots & \vdots & \vdots & \vdots & \vdots & \vdots & \vdots & \ddots \end{pmatrix} \tag{9}$$

$$H_{JC} = \hbar\omega_a \begin{pmatrix} -\frac{1}{2} & 0 & 0 & 0 & 0 & 0 & 0 & 0 & \dots \\ 0 & \frac{1}{2} & 0 & 0 & \frac{\lambda}{\omega_a} & 0 & 0 & 0 & \dots \\ 0 & 0 & \frac{3}{2} & 0 & 0 & \frac{\lambda\sqrt{2}}{\omega_a} & 0 & 0 & \\ 0 & 0 & 0 & \frac{5}{2} & 0 & 0 & \frac{\lambda\sqrt{3}}{\omega_a} & 0 & \dots \\ 0 & \frac{\lambda}{\omega_a} & 0 & 0 & \frac{1}{2} & 0 & 0 & 0 & \dots \\ 0 & 0 & \frac{\lambda\sqrt{2}}{\omega_a} & 0 & 0 & \frac{3}{2} & 0 & 0 & \dots \\ 0 & 0 & 0 & \frac{\lambda\sqrt{3}}{\omega_a} & 0 & 0 & \frac{5}{2} & 0 & \dots \\ 0 & 0 & 0 & 0 & 0 & 0 & 0 & \frac{7}{2} & \dots \\ \vdots & \vdots & \vdots & \vdots & \vdots & \vdots & \vdots & \vdots & \ddots \end{pmatrix} \tag{10}$$

There are actually a number of ways in which the Hamiltonian can be represented in matrix form with each form being valid and yielding the same results. Each form will use the same matrix elements but in a different arrangement. Interested readers could observe the form in Irish [7] as an example. Using these matrices, we computed the eigenvalues for both the RWA and the non-RWA Hamiltonians. We also evaluated how the probability of finding the system in an excited state,$P_e(t)$, varies over time by using the the time evolution operator [2]

$$U(t) = e^{-iHt/\hbar} \tag{11}$$

and applying it to an initial state $|e\rangle |n\rangle$, where n is a specific number state, to then calculate the probability

$$P_e(t) = \sum_{m=0}^{\infty} |\langle m| \langle e| U |e\rangle |n\rangle|^2 \tag{12}$$

which is the sum of the probabilities of finding the state in an excited state for any number state, m, after time t. In reality we will use an upper limit of m equal to that of the size of the Hamiltonian matrix that we are using while ensuring that the matrix is large enough so that the finite nature of the matrix does not interfere significantly with the results for the initial number states we are considering. We then repeated this for an initial coherent state, α, which we know is related to the number states by [2]

$$|\alpha\rangle = \sum_{n=0}^{\infty} \frac{\alpha^n}{\sqrt{n!}} e^{-\frac{|\alpha|^2}{2}} |n\rangle \tag{13}$$

1 Part A: How the Eigenvalues Change when Varying λ/ω

1.1 Results

The results shown in 1 were obtained by calculating the eigenvalues of a finite 40×40 matrix for both the full Hamiltonian and the Jaynes-Cummings model Hamiltonian over varying λ/ω_a values.

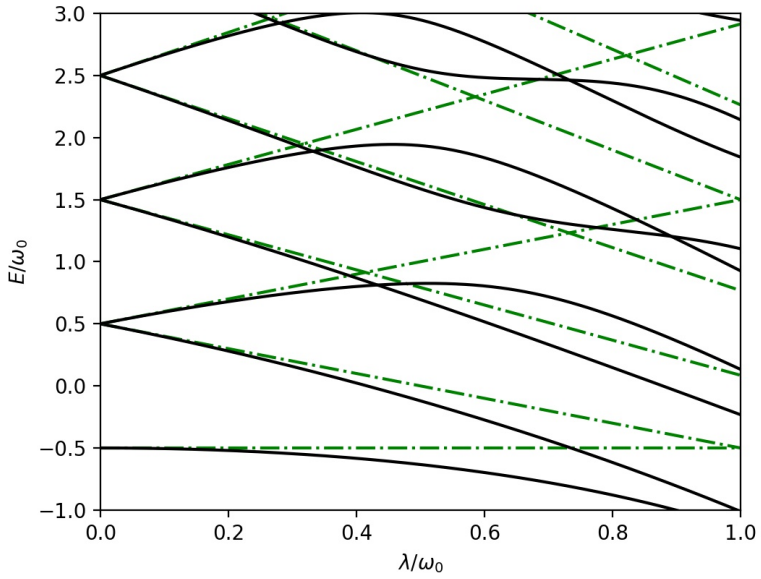

Figure 1: How the eigenstates change for various λ/ω_a. This graph shows the energy eigenvalues when varying λ/ω_a for the full Hamiltonian (solid black line), and the Hamiltonian using the RWA (dotted dashed green line). These values appear to be different depending on whether or not we take the rotating wave approximation.

1.2 Discussion

Figure 1 shows that the rotating wave approximation is good for small values of λ/ω_a. The system is approximated well for small values, but as the value of λ/ω_a is increased, we see that the rotating wave approximation diverges from the numerically determined eigenvalues of the system when not using the RWA. The RWA appears to give a very good approximation up until $\lambda/\omega_a = 0.1$ and a good approximation up until $\lambda/\omega_a = 0.2$. These results agree with those found in Irish [7], so we can have good confidence that these results are accurate and that the Hamiltonian matrices have been constructed in a valid manner.

2 Part B: How the System Evolves Over Time

2.1 Results

The following results show the probability in finding the system in an excited state after time, $\omega_a t$. We use this dimensionless time as we have not defined an actual value for ω_a but we are instead using a ratio of λ/ω_a in the matrices and so we can see from equations 9 and 10 that a factor of ω_a is present which will be involved in the time evolution operator in equation 11. Figure 2 shows the result when $n = 0$ and $\lambda/\omega_a = 0.1$ for both the RWA case and the non-RWA case.

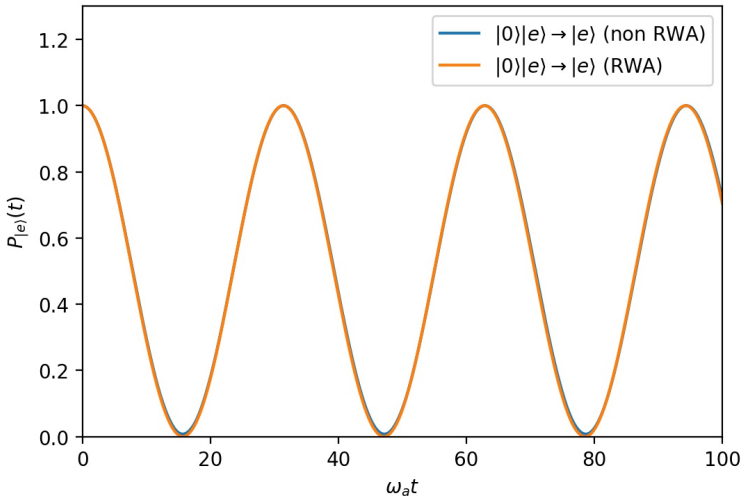

Figure 2: When $\lambda/\omega_a = 0.1$, the discrepancy between graphs where the RWA is used and where it is not is very small.

We can see that the expected $\cos^2(t\omega_{\text{result}})$ is produced where ω_{result} is the dimensionless frequency at which the probability wave oscillates. We measured the period, $T\omega_a$, and calculated the frequency of the wave and found the form in which the result matches that in equation 1 where $\omega_{\text{result}} = \lambda\sqrt{n+1}$. Table 1 shows these results for $\lambda = 0.1$ for the RWA case.

Initial state, n	$T\omega_a \pm 0.010$	ω_{result}	Form
0	31.413	0.100008 ± 0.000032	$\lambda\sqrt{1}$
1	22.213	0.141430 ± 0.000064	$\lambda\sqrt{2}$
2	18.137	0.173215 ± 0.000096	$\lambda\sqrt{3}$
3	15.707	0.20002 ± 0.00013	$\lambda\sqrt{4}$
4	14.050	0.22360 ± 0.00016	$\lambda\sqrt{5}$

Table 1: Change in measured period of the probability wave, $T\omega_a$, calculated frequency of the wave,ω_{result}, and form of result from varying n when using the RWA

Table 2 is similar and shows the results for a constant number state and a varying λ for $n = 0$ in the RWA case.

λ	$T\omega_a \pm 0.010$	ω_{result}	Form
0.05	62.830	0.0499379 ± 0.0000080	$\lambda\sqrt{1}$
0.10	31.413	0.100008 ± 0.000032	$\lambda\sqrt{1}$
0.15	20.940	0.150028 ± 0.000072	$\lambda\sqrt{1}$
0.20	15.707	0.20002 ± 0.00013	$\lambda\sqrt{1}$
0.25	12.567	0.24999 ± 0.00020	$\lambda\sqrt{1}$
0.30	10.473	0.29996 ± 0.00029	$\lambda\sqrt{1}$
0.35	8.977	0.349973 ± 0.00039	$\lambda\sqrt{1}$
0.40	7.853	0.400033 ± 0.00051	$\lambda\sqrt{1}$
0.45	6.980	0.450085 ± 0.00064	$\lambda\sqrt{1}$
0.50	6.283	0.499988 ± 0.00080	$\lambda\sqrt{1}$

Table 2: Change in measured period of the probability wave, $T\omega_a$, calculated frequency of the wave, ω_{result}, and form of result from varying λ when using the RWA

The uncertainty in the period measurement,$\delta(T\omega_a)$, was based on the resolution of the time axis in the

simulation. The uncertainty in the frequency values, $\delta\omega_{\text{result}}$, were calculated based on the uncertainty of the period using the uncertainty propagation equation

$$\delta\omega_{\text{result}} = \pi \times \frac{\delta T \omega_a}{(T\omega_a)^2} \tag{14}$$

We then explored what effect increasing the value of λ/ω_a had on the results from figure 2 and these results are shown in figures 3 and 4.

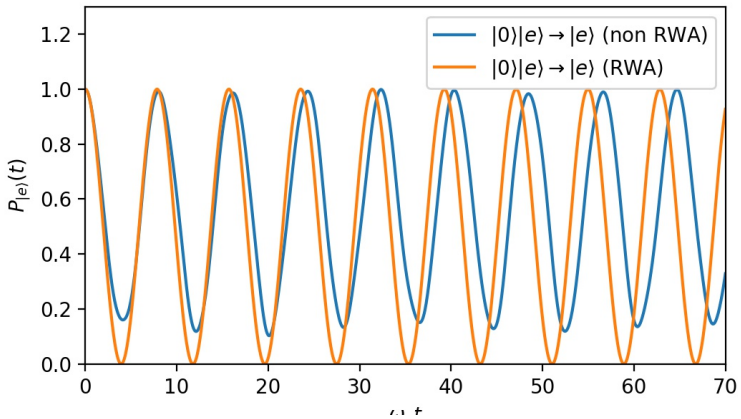

Figure 3: When $\lambda/\omega_a = 0.4$, the discrepancy is getting larger.

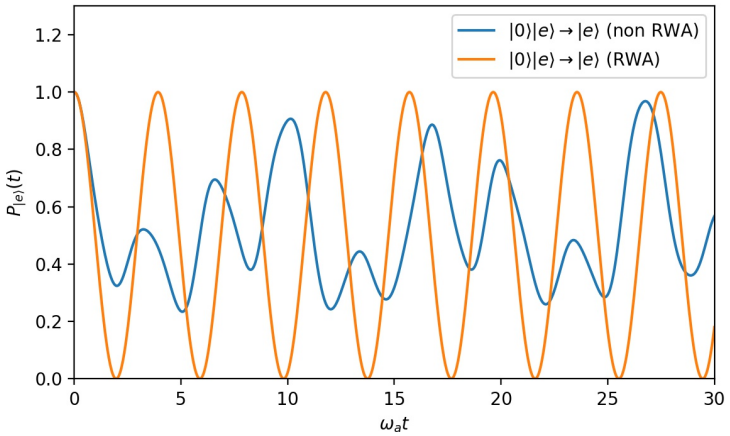

Figure 4: $\lambda/\omega_a = 0.8$. As we are increasing the value of λ/ω_a, the RWA and non-RWA graphs diverge from each other.

We also then explored the effect of changing the initial number state while at a much larger λ/ω_a value. Figure 5 shows the RWA case for $n = 0$ and $n = 3$ at $\lambda/\omega_a = 2$ while figure 6 shows the same for the non-RWA case.

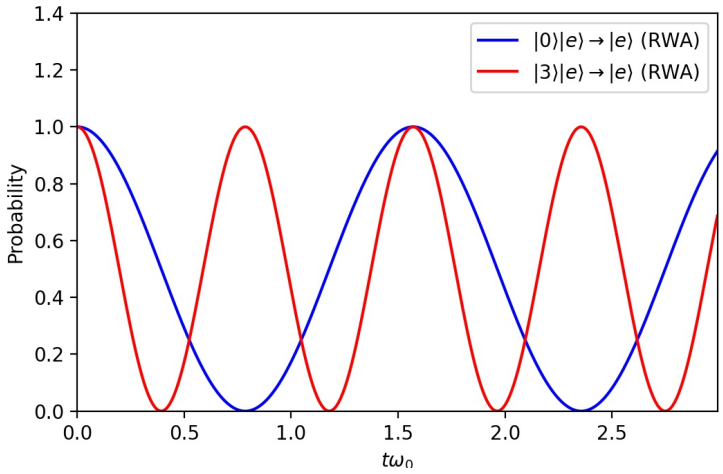

Figure 5: Evolution of states $|n\rangle |e\rangle$ for $n = 0$ and $n = 3$. Here $\lambda/\omega_a = 2$, but when using the RWA, this only affects the frequency.

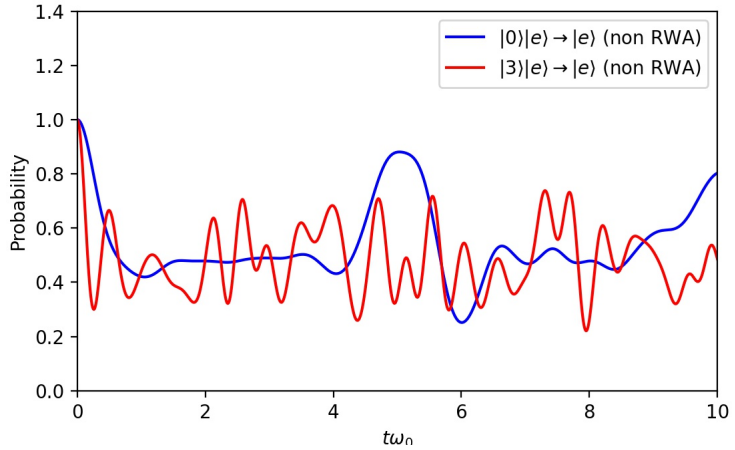

Figure 6: The same graph as 5, but without making the RWA. $\lambda/\omega_a = 2$.

2.2 Discussion

We see some trends when varying the values of λ/ω_a and n. Firstly, we can see that the RWA is a good approximation for the case where $\lambda/\omega_a \ll 1$ (see Figure 2). However, we can see from Figures 3 and 4 that as we increase λ/ω_a, the RWA diverges greatly from the full Hamiltonian. To understand why this is, we can look at the Hamiltonian given in equation 2. If we look at this equation, we can see that the last term affects the $|g\rangle$ and $|e\rangle$ kets (having the $\hat{\sigma}_+$ and $\hat{\sigma}_-$ operators). When we make the rotating wave approximation, we are removing the $\hat{\sigma}_- \hat{a}^\dagger$ and $\hat{\sigma}_+ \hat{a}$ operators. These terms have λ as a coefficient, so when we increase λ/ω_a, the contribution of the removed terms to the effects of the Hamiltonian increases, and therefore there is a greater discrepancy between the full Hamiltonian and the RWA.

Now let's look at what happens when we increase the value of n for high values of λ/ω_a. We can see from Figure 5 that with the rotating wave approximation, the frequency increasing is the only effect, with otherwise identical graphs being produced. It increases proportionally to $\sqrt{n+1}$, as we can see from Table 1. For the rotating wave approximation, we still have a random looking wave, but we can see that the frequency is higher for higher values of n (see Figure 6).

We have also demonstrated that the frequency of the produced wave when using the RWA is proportional to $\lambda\sqrt{n+1}$, as shown in Tables 1 and 2.

3 Part C: The dynamics of coherent states

3.1 Results

The results in figures 7-14 show a similar set of results to those in the previous section but for the case where we start in an initial coherent state $|\alpha\rangle\,|e\rangle$.

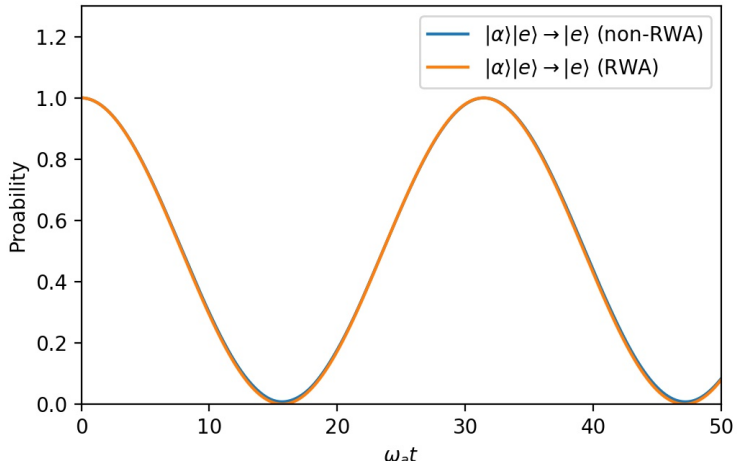

Figure 7: When we start in the coherent state with $\alpha = 0$ and $\lambda/\omega_a = 0.1$, we get similar results to part B, with the same frequency as if we had started in the state $|0\rangle\,|e\rangle$.

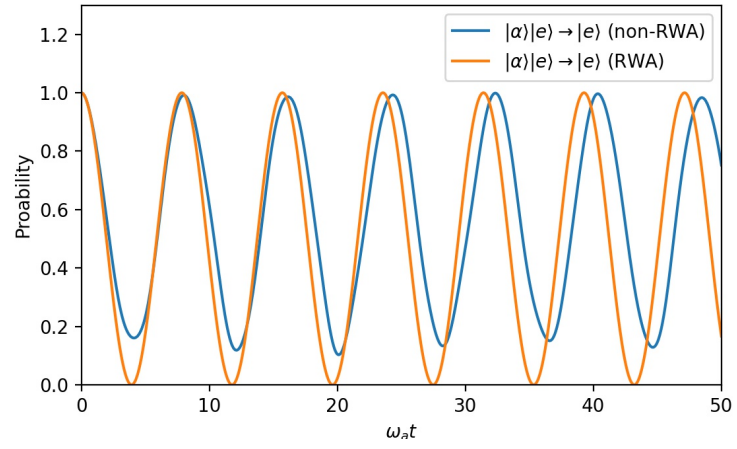

Figure 8: $\alpha = 0$ and $\lambda/\omega_a = 0.4$. The RWA looks similar to Figure 3, but the full Hamiltonian graph deviates more.

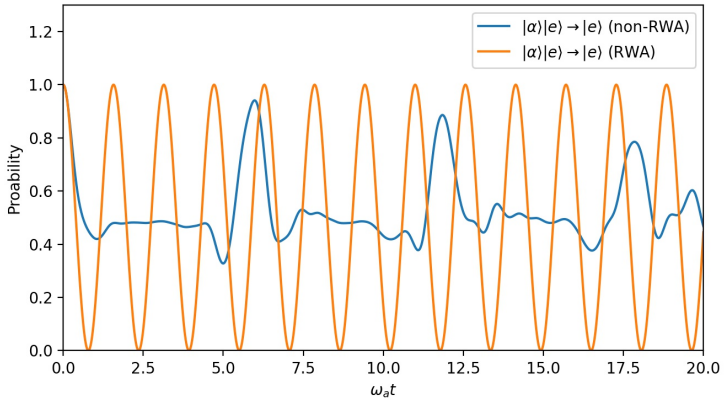

Figure 9: $\alpha = 0$ and $\lambda/\omega_a = 2.0$. Now the RWA is much different to the full Hamiltonian. We can see spikes approximately every $6\omega_a t$ in the non RWA case.

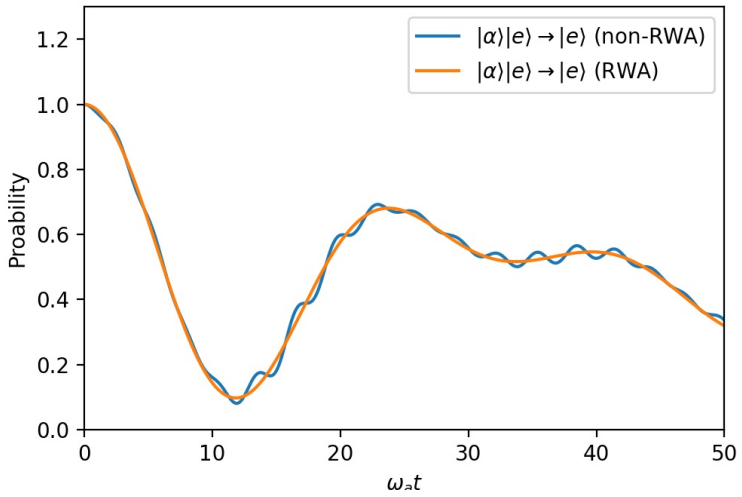

Figure 10: $\lambda/\omega_a = 0.1$, $\alpha = 1$. We can see that the RWA gets the general idea of the system, but doesn't show all the small oscillations found within the larger ones.

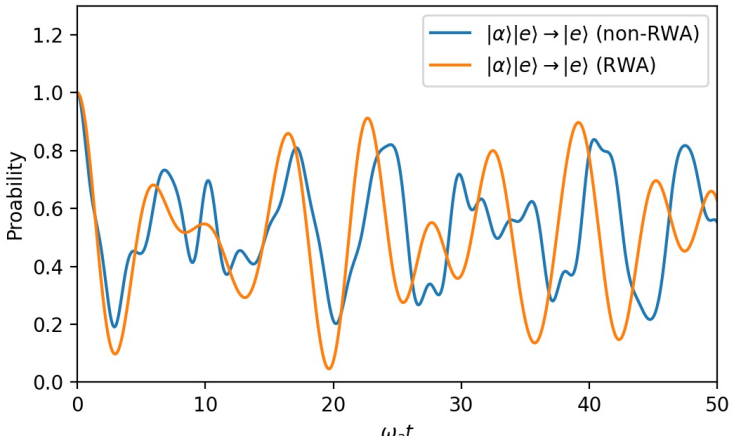

Figure 11: $\lambda/\omega_a = 0.4$, $\alpha = 1$. When we increase the value of λ/ω_a, we can see the RWA start to drift away from the true time evolution.

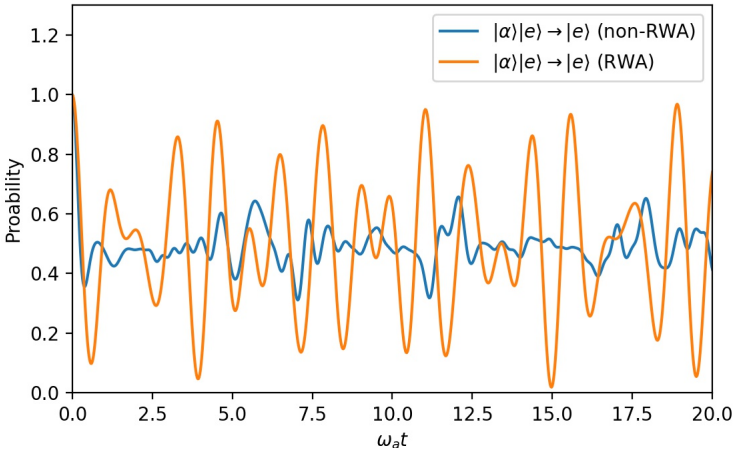

Figure 12: $\lambda/\omega_a = 2.0$, $\alpha = 1$. Now the RWA is very far away from the true graph.

We also see some interesting effects where the time evolution of the system looks like wave packets.

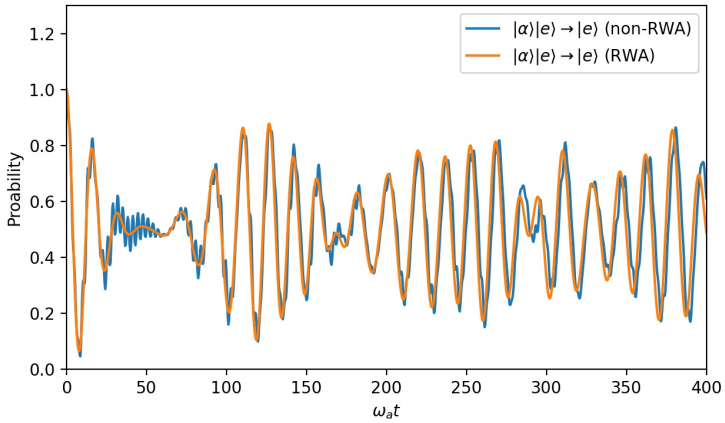

Figure 13: $\lambda/\omega_a = 0.1$, $\alpha = 3$. For this graph, I have set the time axis to run to $t/\omega_a = 400$. We start to see an interesting shape occur: it appears that there are wave packets.

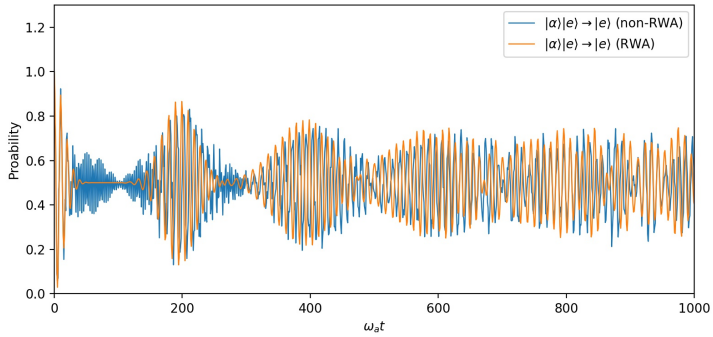

Figure 14: $\lambda/\omega_a = 0.1$, $\alpha = 9$. Here, α is to a much higher value and now we can clearly see the wave packets. The RWA has a similar shape but the wave packets occur earlier on.

3.2 Discussion

Let's first take a look at Figures 7, 8 and 9, which all show graphs of the system when $\alpha = 0$. Starting with the case where $\lambda/\omega_a = 0.1$, the RWA and full Hamiltonian align very closely. They have the same frequency as Figure 2, where the system starts in the $|0\rangle|e\rangle$ state. When λ/ω_a is increased to 0.4, the full Hamiltonian starts to drift away from the RWA. When $\lambda/\omega_a = 2.0$, the RWA carries on increasing in frequency in the same way proportionally to λ/ω_a, but the full Hamiltonian produces a very different graph. There is not much oscillation, but interestingly, we see peaks every 6 units of time. This is due to the collapse and revival cycle described in Section 3.2.1, and similar results can be seen in [3].

Let's now look at the case where $\alpha = 1$. We see from Figures 10, 11 and 12 that as λ/ω is increased, the RWA and non-RWA graphs diverge from each other. When $\lambda/\omega_a = 0.1$, the two graphs align very closely and the RWA models the general shape of the full Hamiltonian very well, but the full Hamiltonian has extra oscillations which the RWA does not show. From Figures 11 and 12, we can see that as λ/ω_a is increased, the graphs drift apart, and also the full Hamiltonian doesn't tend to oscillate with as high of an amplitude as the RWA case.

3.2.1 Collapse and Revival

Finally, let's look at what happens when we increase α even further, setting $\lambda/\omega_a = 0.1$. In Figure 13, we can start to see an interesting pattern emerge: the waves for both the RWA and the full Hamiltonian start to look like wave packets. This can be seen much more dramatically when we increase the value of α even higher to $\alpha = 9$, shown in Figure 14: we can see very distinct wave packets. After the first two wave packets, the wave packets are not as apparent.

Note that in this graph, the rotating wave approximation has wave packets appearing earlier than the full Hamiltonian. Note also that the RWA hardly moves from being 0.5 in the early portion of the graph, from around $t = 30$ to $t = 170$.

These wave packets are known as collapses and revivals [3]. Experimentally, these collapses and revivals were first observed by Rempe et al. [8], using the interaction of a single Rydberg atom with a single mode of an electromagnetic field in a superconducting cavity. When the Jaynes-Cummings model is evaluated analytically, the collapses and revivals can be seen. These collapses and revivals are distinctly quantum features and do not occur in the classical model [8]. This is due to the fact that our coherent state $|\alpha\rangle$ is made up of an infinite sum of number states $|n\rangle$, which Rabi oscillate at different frequencies depending on the value of n. These will fall out of phase, causing a collapse. After some time, the states come back into phase, causing a revival [3]. These collapses and revivals were investigated by J. H. Eberly et al. [9] and our results show resemblance to these.

4 Conclusion

We have used the Jaymes-Cummings model to investigate how well the RWA holds when compared with the full Hamiltonian which fully describes the system. When looking at the energy eigenvalues of the system, we have shown that the rotating wave approximation diverges from the full Hamiltonian as the coupling strength is increased in a manner that agrees with the literature [3]. By starting the system in the $|n\rangle|e\rangle$ state for various values of n, we have shown the divergence of the RWA from the full Hamiltonian in the strong coupling regime, for which the RWA is no longer a valid model to describe the behaviour of this system. We have demonstrated that when using the RWA, the probability of the system being in the excited state oscillates with a frequency proportional to $\lambda\sqrt{n+1}$. Finally, we investigated the behaviour of the system when prepared in the coherent state $|\alpha\rangle|e\rangle$. We found that for low values of λ, the rotating wave approximation approximated the general shape of the system, but when using the Hamiltonian, we find that there are extra, much smaller oscillations which cannot be seen when using the RWA. We also showed that when α is very high, the system undergoes collapses and revivals as predicted by the Jaymes-Cummings model [1]. When using the RWA, we see that the probability of finding the system in the excited state almost completely stops oscillating and remains at 0.5 for a long amount of time before the revival occurs. However, when using the Jaynes-Cummings Hamiltonian, we see that this picture is not entirely accurate and, although both models show collapses and revivals, the rotating wave approximation shows a different pattern to the non rotating wave approximation case. The RWA is no longer a valid approximation for some experiments which have produced strong coupling [4–6], so it is important to understand the behaviours of strongly coupled systems without relying on the RWA.

References

[1] E.T. Jaynes and F.W. Cummings. Comparison of quantum and semiclassical radiation theories with application to the beam maser. *Proceedings of the IEEE*, 51(1):89–109, 1963. ISSN 0018-9219.

[2] C. C. (Christopher C.) Gerry. *Introductory quantum optics / Christopher Gerry, Peter Knight.* Cambridge University Press, Cambridge, 2005. ISBN 0521820359.

[3] Jonas Larson. Dynamics of the jayne-cummings and rabi models: old wine in new bottles. *arXiv.org*, 2007. ISSN 2331-8422.

[4] Xiu Gu, Anton Frisk Kockum, Adam Miranowicz, Yu-xi Liu, and Franco Nori. Microwave photonics with superconducting quantum circuits. *Physics reports*, 718-719:1–102, 2017. ISSN 0370-1573.

[5] P. Forn-Díaz, L. Lamata, E. Rico, J. Kono, and E. Solano. Ultrastrong coupling regimes of light-matter interaction. *Reviews of modern physics*, 91(2):025005, 2019. ISSN 0034-6861.

[6] Fumiki Yoshihara, Tomoko Fuse, Sahel Ashhab, Kosuke Kakuyanagi, Shiro Saito, and Kouichi Semba. Superconducting qubit-oscillator circuit beyond the ultrastrong-coupling regime. *Nature physics*, 13(1):44–47, 2017. ISSN 1745-2473.

[7] E.K. Irish. Generalized rotating-wave approximation for arbitrarily large coupling. *Physical review letters*, 99(17):173601–173601, 2007. ISSN 0031-9007.

[8] Gerhard Rempe, Herbert Walther, and Norbert Klein. Observation of quantum collapse and revival in a one-atom maser. *Phys. Rev. Lett.*, 58:353–356, Jan 1987. doi: 10.1103/PhysRevLett.58.353. URL https://link.aps.org/doi/10.1103/PhysRevLett.58.353.

[9] J. H. Eberly, N. B. Narozhny, and J. J. Sanchez-Mondragon. Periodic spontaneous collapse and revival in a simple quantum model. *Phys. Rev. Lett.*, 44:1323–1326, May 1980. doi: 10.1103/PhysRevLett.44.1323. URL https://link.aps.org/doi/10.1103/PhysRevLett.44.1323.